

Design and Implementation of Geophysical Monitoring and Remote Sensing during a Full Scale Embankment Internal Erosion Test

Michael A. Mooney¹, Minal L. Parekh¹, Ben Lowry², Justin Rittgers³, Jacob Grasmick¹, André R. Koelewijn⁴, André Revil^{3,5}, Wendy Zhou²

¹Civil and Environmental Engineering, Colorado School of Mines, Golden, Colorado, United States.

²Geology and Geological Engineering, Colorado School of Mines, Golden, Colorado, United States.

³Geophysics, Colorado School of Mines, Golden, Colorado, United States

⁴Deltares, Delft, Netherlands

⁵IS Terre, CNRS, UMR CNRS 5275, Université de Savoie, Le Bourget du Lac, France

ABSTRACT

This paper describes the conception and deployment of a multi-geophysics and remote sensing approach to monitoring internal erosion in a test embankment that was loaded and brought to failure in Booneschans, Netherlands in fall 2013. IJkdijk is a full-scale field testing embankment constructed to facilitate sensor validation testing for monitoring embankment loading and failure conditions. The embankment was constructed of a single zone high plasticity clay embankment with sand foundation. The test embankment was subjected to reservoir loads simulating tidal and storm surge conditions known to induce internal erosion in actual embankments. Geophysical monitoring of subsurface conditions was pursued using self-potential and passive seismic methods. Concurrent terrestrial lidar remote sensing methods was implemented to track millimeter scale deformation. Each of these monitoring approaches was implemented successfully and yielded useful spatial and temporal information throughout the seven days of testing, from initial reservoir loading to completion of the test.

INTRODUCTION

Earth dams and levees (EDLs) provide flood protection, clean water supply and renewable energy for millions to billions of people worldwide. As they age and are subjected to increased load and demand, continued reliable performance is a concern. Inevitably, water flows or seeps through EDLs and this seepage, if uncontrolled, can lead to internal erosion. Internal erosion is one of the primary processes threatening the structural health of earthen embankments yet the mechanisms involved and opportunities to detect the process are not yet well understood (Schmertmann 2000, Beek et al. 2010).

Internal erosion results from the transport and migration of soil particles subject to focused seepage or leakage flow and can occur in the embankment, through the foundation and from the embankment into the foundation. Of particular interest here, backward erosion occurs where cohesionless soils are subject to seepage uplift pressures that cause the soils to float or heave and manifest as sand boils in surface expression, generally at the downstream toe of a dam. The detached particles are carried away by the seepage flow and the process back-propagates until forming a continuous path (“pipe”) to the upstream reservoir. Detection of internal erosion when it manifests on the surface as a boil or sinkhole is too late, yet methods of detection other than visual inspection performed from the surface of a structure are not part of current monitoring practice. In the context of large-scale monitoring systems for earth dams and/or levees, the periodic implementation of conventional geophysical surveys using active seismic or current sources is ill-timed compared with the rapid deterioration of levees via internal erosion. There is a need for more continuous time-lapse geophysical methods for monitoring EDLs.

This paper focuses on the conception and deployment of a multi-geophysics and remote sensing approach to monitoring internal erosion in a test embankment that was loaded and brought to partial failure in Booneschans, Netherlands in fall 2013. The IJkdijk (pronounced “ike dike” and Dutch for “calibration levee”) is a field facility where full-scale levees have been constructed and loaded since 2007 to study levee behavior and to enable testing of sensor technologies for monitoring behavior and technologies for mitigation (see <http://www.ijkdijk.nl/en/>). A continuous monitoring system involving passive electric, passive seismic and acoustic emissions, and terrestrial remote sensing with lidar was conceptualized and implemented over a seven day period of loading and partial failure of the embankment levee. The paper describes the IJkdijk embankment and loading schedule, the geophysical and remote sensing approaches used, and the design of the monitoring approach implemented. Some preliminary results are presented.

DESCRIPTION OF TEST LEVEE

The test embankment shown in cross section on Figure 1 was 18 m long at its base and 27 m long at the crest. The embankment consists of moisture-conditioned and compacted homogeneous high plasticity clay over a poorly graded sand foundation (see Table 1). The embankment and sand foundation were constructed over a geomembrane to isolate the test from the influence of outside soil and groundwater, as shown in Figure 1. The facility included a membrane-lined upstream reservoir to provide hydraulic loading on the embankment and a membrane-lined constant-head downstream reservoir. The downstream reservoir was equipped with an outflow gaging station. The foundation sands were saturated prior to the start of any hydraulic loading. The test included installation of a vertically-oriented geotextile strip near the downstream toe of the embankment as a potential internal erosion mitigation method, shown in Figure 1. This paper does not specifically address the influence of the geotextile on the behavior of the embankment. The embankment was instrumented with piezometers at locations described in Figure 1, generally spaced at 1.5 m into the page except at the upstream toe.

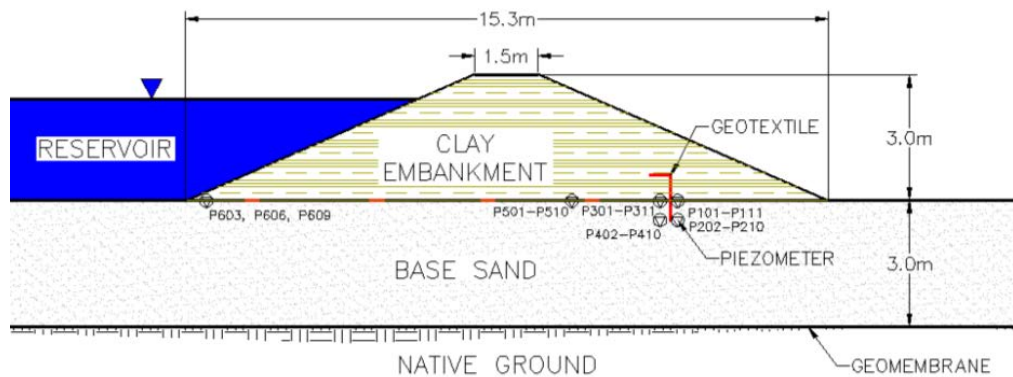


Figure 1 IJkdijk test embankment cross section.

Table 1. Summary of embankment soil properties

Embankment Clay	w (%)	LL	PL	PI	$\% > 63 \mu\text{m}$	Unit weight (kN/m^3)
	45-65	79-89	26-33	52-61	3-9	15.2-16.1

	d_{85}	d_{70}	d_{50}	d_{15}	C_u
Foundation Sand (upper 0.5 m)	0.23	0.21	0.18	0.12	1.7
Foundation Sand (lower 2.5 m)		0.18	0.16		1.6

The hydraulic loading was accomplished by pumping water from a nearby ditch into the upstream reservoir. The loading schedule is shown in Figure 2. The levee exhibited visual signs of deformation, seepage on the downstream face, and sand boils at the toe. While not the subject of this paper, the visual observations of these items are noted in Figure 2.

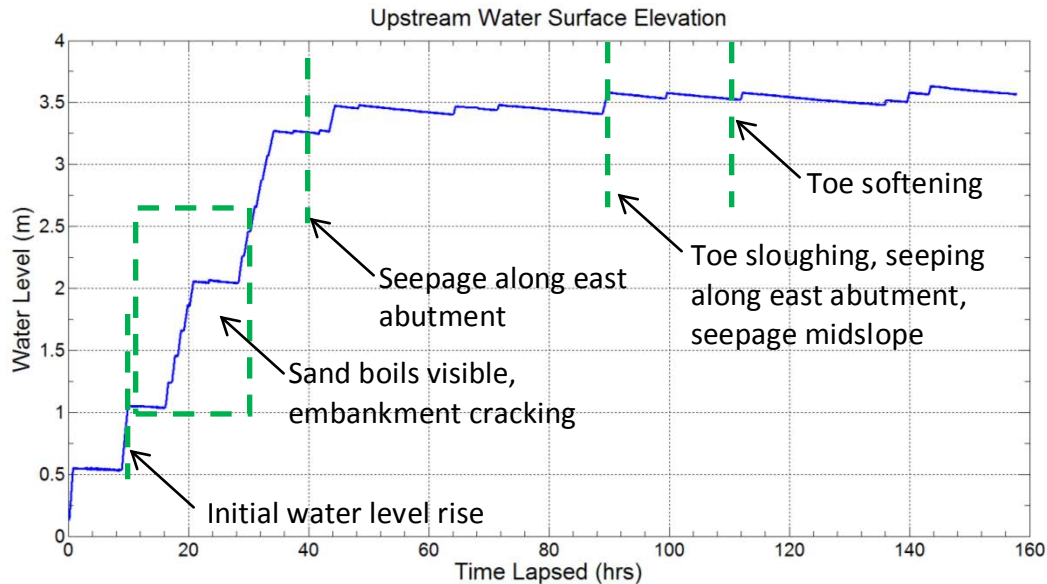


Figure 2 Hydraulic loading schedule and visual surface observations

GEOPHYSICAL AND REMOTE SENSING MONITORING SCHEME

Passive Electric – Self-Potential (SP)

The self-potential (SP) method is a passive geophysical method (no current injection required) that measures naturally occurring or anthropogenic changes to the electrical field generated by electrical source current mechanisms within the subsurface. Common source contributions to observed self-potential signals can include spatial gradients in hydraulic potential, temperature, and chemical or ionic concentrations. These sources result in various cross-coupled electrical source currents such as electrokinetic, thermoelectric, and electrochemical currents (Jardani et al. 2010; Minsley et al. 2007; Revil et al. 2012; Sheffer 2007).

In very general terms, seepage through an embankment will typically create a dipolar or bipolar SP signature with a positive pole on the downstream side and the corresponding negative pole on the upstream side. To image subtle fluctuations in the electrical field that result from fluid flow through and below the test structure, a 74 electrode array was designed and implemented, including 57 Pb-PbCl non-polarizable electrodes on the downstream face and 17 electrodes across the upstream face of the test structure (see Figure 3). This array was designed to capture the SP fluctuations on

each side of the structure in order to invert these fluctuations in terms of preferential ground water flow pathways. The SP electrodes were installed approximately 0.75m below ground surface to minimize diurnal temperature fluctuations and drifts of the electrodes and to improve the proximity of the electrode array to any possible seepage pathway locations. SP data were recorded using a laptop connected via Ethernet to a Keithley 2700 series digital multimeter with multiplexed slot cards supporting a total of 80 analog input channels. The system was configured to cycle through each electrode and record an SP measurement each 0.5 sec, enabling the electric field distribution across the test structure to be imaged approximately every 40 sec

Passive Seismic -Acoustic Emissions

An array of 24 geophones was deployed on the downstream face to passively record vibrations throughout the test. The recorded signal may include acoustic emissions (AE) from collapse events, movement of water, movement of particles (DiCarlo et al. 2003; Hickey et al. 2010; Hung et al. 2009) and may include wave propagation from various ‘noise’ sources, e.g., vehicle traffic, foot traffic. The seismic system recorded nearly continuously in 16-sec records (approximately 4 sec downtime between records) using a 24-channel Geometrics Geode seismograph. The sensor layout was designed to capture and record seismic energy propagating across the geophone array and up to the ground surface, including any AE events that may have occurred during the test. The sensors used were 4.5 Hz Mark Products vertical geophone transducers. A 4 kHz sample rate (per sensor) was used for the first three days, but was reduced to 1 kHz for the remaining three days due to software issues. Each geophone was buried 0.25 - 0.75 m deep to maximize coupling and sensitivity to signals of interest while minimizing the negative impacts of random and high-energy vibrations from wind and rain.

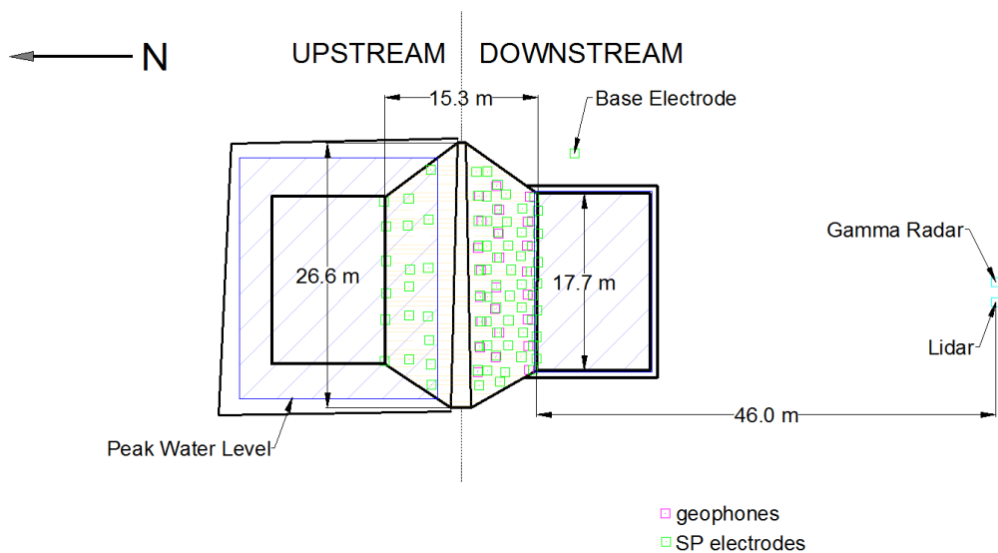


Figure 3. Plan view of geophysical sensor arrays and lidar imaging location

Remote Sensing

Some deformation of an EDL is expected with hydraulic loading, but localized deformation on an embankment face can indicate incipient failure conditions like sinkhole development, slope failures, and liquefaction (United States Bureau of Reclamation et al. 2007). Terrestrial remote sensing sensors for light detection and ranging (LiDAR) and radar interferometry were deployed to support monitoring efforts of the embankment. Only LiDAR is described here. Ground based LiDAR is capable of resolving ground surface movement on a scale of millimeters or less (Abellán et al. 2009; Alba et al. 2008).

LiDAR point clouds were acquired using a Leica C10 with a green laser light and self-leveling sensor at a sampling interval of 7 min. for the duration of the test. Deformation mapping was conducted on a 5 cm grid of the embankment using lowest return grid creation. Repeated time series of elevation grids were differenced to obtain a vertical difference grids. Vertical differencing is effective at detecting changes on the embankment but is acknowledged to only represent the vertical component of movement. 3D ground surface deformation can capture the complex movements but is not processed in this analysis. Near horizontal deformation is detected by the radar sensor.

For the duration of the testing program, the absolute 3D spatial locations of all pertinent data locations, including geophones, seismic sources, and resistivity electrodes, and structure apexes were recorded using real time kinematic GPS. Precise location is important for minimizing introduction of error into inverse modeling routines, which can be sensitive to minute errors in geometries and other data variations.

PRELIMINARY MONITORING RESULTS

The complete analysis and presentation of the data is ongoing and not the focus of this paper; however, some preliminary data from self-potential, acoustic emission, and lidar are presented here to illustrate the nature of each imaging approach.

Self-Potential

Figure 4 presents a three image sequence of downstream face electrical potential around $t = 100$ hrs to illustrate the capabilities of this technique. The SP data from 57 downstream face electrodes were gridded and interpolated. SP data have been processed to remove baseline steady-state potentials and to correct for drift that often occurs with field-deployed electrodes. As illustrated in Figure 4, the SP images reveal the development of a small magnitude ($\sim 4\text{mV}$) positive anomaly at the center of the downstream toe. This anomaly was consistent with a large sand boil that developed during this time.

Acoustic Emission

A simple way to characterize AE activity is to count pulses or peaks larger than a threshold energy or voltage level. The threshold level is set somewhat arbitrarily and

is often determined based on noise levels collected prior to hydraulic loading. Figure 5 illustrates this approach by presenting observed counts above a threshold during two 16 sec windows of time during the test. Figure 5a shows counts recorded early during the test at low reservoir loading ($t = 16$ hrs) and Figure 5b shows counts at high reservoir loading ($t = 112$ hrs).

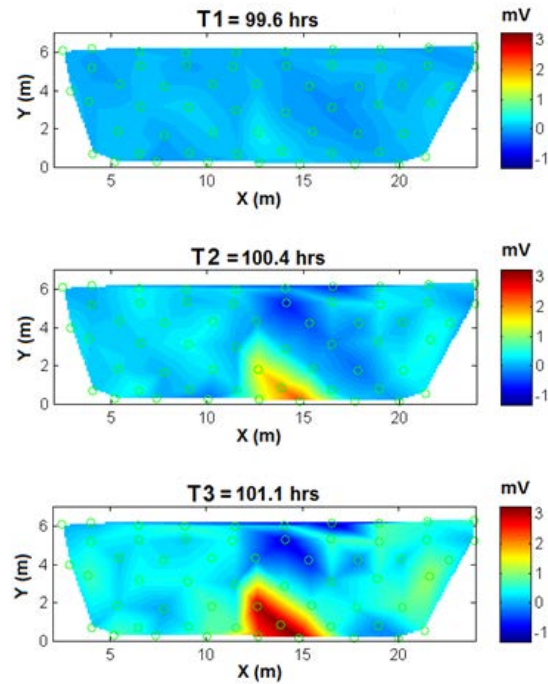


Figure 4. SP data collected near $t = 100$ hrs illustrating the development of a positive anomaly

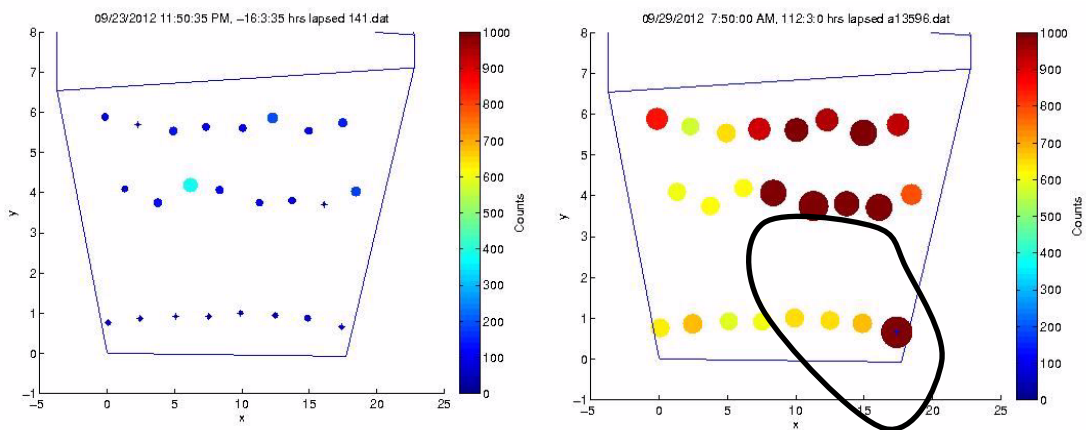


Figure 5. Acoustic emissions during (a) low reservoir elevation at $t = 16$ hrs and (b) at full reservoir loading at $t = 112$ hrs

Terrestrial Remote Sensing

Cumulative vertical deformation at two times are shown in Figure 6. Filling of the reservoir resulted in deformation near the crest on the flanks of the embankment that developed as the reservoir was loaded to capacity at $t = 45$ hrs. These features remain and grow slightly throughout the rest of the test. After 108 hrs, indications of vertical settlement at the toe are apparent, with vertical deformation approaching 15 cm. Some shadowing noise was introduced by the placement of cardboard signs at the toe and observation activities but sufficient imagery was captured to give clear scenes.

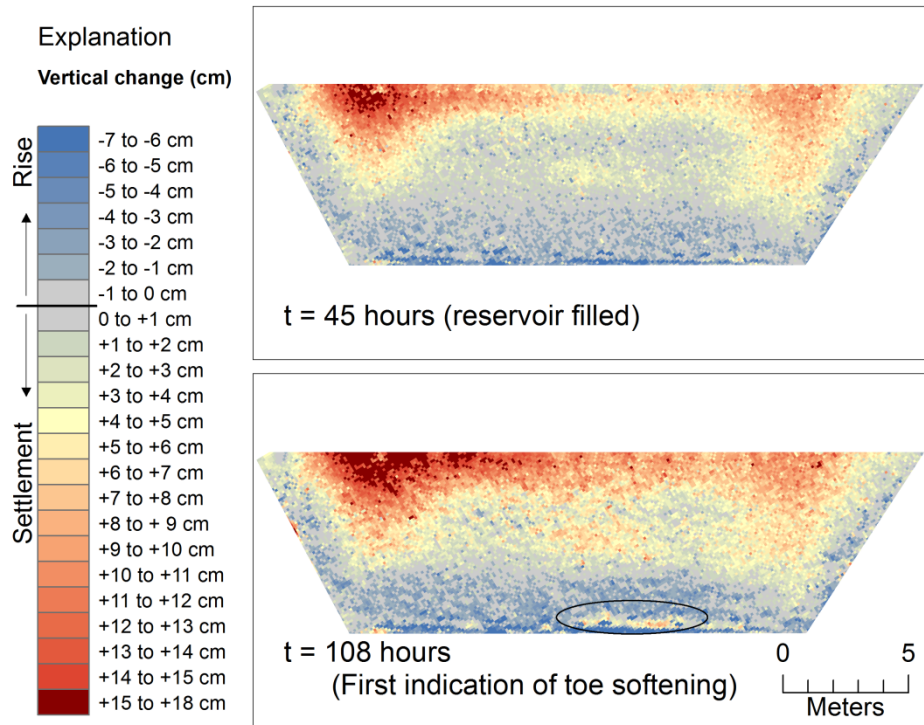


Figure 6. Vertical surface deformation as measured by lidar. Most deformation occurred after reservoir was filled. Toe softening was first observed at 108 hrs.

CONCLUDING REMARKS

A continuous monitoring system involving passive electric, passive seismic and acoustic emissions, and terrestrial remote sensing with lidar was conceptualized and implemented over a seven day period of loading and failure of the IJkdijk test embankment. Each of these monitoring approaches was implemented successfully and yielded useful spatial and temporal information throughout the seven days of testing, from initial reservoir loading to completion of the test. Full analysis of these data sets will determine the true value of each of these noninvasive approaches in better understanding the behavior of embankments from loading through failure.

ACKNOWLEDGEMENTS

Staatsbosbeheer is gratefully acknowledged for providing the test site at Booneschans. The Dutch Ministry of Economic Affairs, Agriculture and Innovation, the Water Board of Rivierenland and the Room for the River program of Rijkswaterstaat are acknowledged for their financial support. The National Science Foundation Partnership for International Research and Education program (grant OISE-1243539) is gratefully acknowledged.

REFERENCES

- Abellán, A., Jaboyedoff, M., Oppikofer, T., and Vilaplana, J. M. (2009). "Detection of millimetric deformation using a terrestrial laser scanner: experiment and application to a rockfall event." *Natural Hazards and Earth System Sciences*, 9(2), 365–372.
- Alba, M., Bernardini, G., Giussani, A., Ricci, P. P., Roncoroni, F., Scaioni, M., Valgoi, P., and Zhang, K. (2008). "Measurement of dam deformations by terrestrial interferometric techniques." *The International Archives of the Photogrammetry, Remote Sensing and Spatial Information Sciences*. Vol. XXXVII. Part B1. Beijing, 133, 139.
- Beek, V.M. van, Knoeff, H. & Sellmeijer, H. 2011. Observations on the process of backward erosion piping in small-, medium- and full-scale experiments, *European Journal of Environmental and Civil Engineering* 15(8), 1115-1137.
- DiCarlo, D. A., Cidoncha, J. I. G., and Hickey, C. (2003). "Acoustic measurements of pore-scale displacements." *Geophysical Research Letters*, Vol. 30(No. 17).
- Gross, H., Jutzi, B., and Thoennessen, U. (2009). "Intensity normalization by incidence angle and range of full-waveform lidar data." *Proc. Commission IV/Int. Arch. Photogramm., Remote Sens. Spatial Inf. Sci*, 405–412.
- Hickey, C., Ekimov, A., Hanson, G., and Sabatier, J. (2009). "Time-Lapse Seismic Measurements on a Small Earthen Embankment During an Internal Erosion Experiment." *SAGEEP 2009 Proceedings*, Keystone, Colorado.
- Hung, M.-H., Lauchle, G. C., and Wang, M. C. (2009). "Seepage-Induced Acoustic Emission in Granular Soils." *Journal of Geotechnical and Geoenvironmental Engineering ASCE*, Vol. 135(No. 4), pp 566–572.
- Jardani, A., Revil, A., Slob, E., and Söllner, W. (2010). "Stochastic joint inversion of 2D seismic and seismoelectric signals in linear poroelastic materials: A numerical investigation." *Geophysics*, 75(1), N19–N31.
- Minsley, B. J., Sogade, J., and Morgan, F. D. (2007). "Three-dimensional self-potential inversion for subsurface DNAPL contaminant detection at the Savannah River Site, South Carolina." *Water Resources Research*, 43(W04429).
- Revil, A., Karaoulis, M., Johnson, T., and Kemna, A. (2012). "Review: Some low-frequency electrical methods for subsurface characterization and monitoring in hydrogeology." *Hydrogeology Journal*, 20(4), 617–658.

- Schmertmann, J. H. (2000). "The No-Filter Factor of Safety Against Piping Through Sands." *Geotechnical Special Publication No. 11 Judgement and Innovation, The Heritage and Future of the Geotechnical Engineering Profession*, 65–132.
- Sheffer, M. R. (2007). "Forward modelling and inversion of streaming potential for the interpretation of hydraulic conditions from self-potential data." PhD Thesis, University of British Columbia.
- United States Bureau of Reclamation, United States Army Corps of Engineers, URS Corporation, and University of New South Wales. (2007). *A Unified Method for Estimating Probabilities of Failure of Embankment Dams by Internal Erosion and Piping-DRAFT*. Version: Alpha.